Pharmaceutical Research, Vol. 25, No. 12, December 2008 (© 2008)
DOI: 10.1007/s11095-008-9639-7

Research Paper

Effect of Surface Energy on Powder Compactibility

Frauke Fichtner,[1] Denny Mahlin,[1,4] Ken Welch,[2] Simon Gaisford,[3] and Göran Alderborn[1]

Received March 6, 2008; accepted May 23, 2008; published online June 12, 2008

Purpose. The influence of surface energy on the compactibility of lactose particles has been investigated.
Materials and Methods. Three powders were prepared by spray drying lactose solutions without or with low proportions of the surfactant polysorbate 80. Various powder and tablet characterisation procedures were applied. The surface energy of the powders was characterized by Inverse Gas Chromatography and the compressibility of the powders was described by the relationship between tablet porosity and compression pressure. The compactibility of the powders was analyzed by studying the evolution of tablet tensile strength with increasing compaction pressure and porosity.
Results. All powders were amorphous and similar in particle size, shape, and surface area. The compressibility of the powders and the microstructure of the formed tablets were equal. However, the compactibility and dispersive surface energy was dependent of the composition of the powders.
Conclusion. The decrease in tablet strength correlated to the decrease in powder surface energy at constant tablet porosities. This supports the idea that tablet strength is controlled by formation of intermolecular forces over the areas of contact between the particles and that the strength of these bonding forces is controlled by surface energy which, in turn, can be altered by the presence of surfactants.

KEY WORDS: amorphous lactose; powder compactibility; surface energy; surfactant; tablet tensile strength.

INTRODUCTION

A pharmaceutical tablet has been described in physical terms (1) as a large cluster of particles, held together by bonds active between external particle surfaces, i.e. the particles bind predominantly by particle–particle adsorption. The fracturing of a tablet involves the separation of the external particle surfaces from each other. Thus, the properties of the surface of the particles should have a significant effect on the tensile strength of the tablet. An important example (1) of the role the particle surface for tablet strength is the marked difference in compactibility between a lubricated, i.e. a powder for which a lubricant is spread out on the particle surfaces, and a non-lubricated powder.

According to continuum fracture mechanics, the tensile strength of a solid is dependent on the microstructure of the solid specimen. The principles of fracture mechanics have been applied to the fracturing of agglomerates and compacts, i.e. porous solid specimens composed of particles surrounded by a network of pores (2–4). In such expressions, the fracture energy of the solid together with the microstructure of the compact (flaw size, agglomerate packing fraction and particle diameter) control agglomerate strength. It is reasonable that the fracture energy will show some proportionality with the surface energy of solids with similar microstructure.

Rumpf's approach (5) to assess tensile strength of agglomerates is based on a bond summation approach, i.e. the strength equates the sum of all inter-particulate forces in the fracture plane (that are separated simultaneously). In case of van der Waals attractions acting between particles, the inter-particulate bonding force is suggested to be proportional to the Hamaker constant, the latter being proportional to the surface energy of the solid (6). Thus, in the case of a bond summation approach, a direct proportionality between tablet strength and surface energy is to be expected.

Irrespective of the conception used to describe tablet strength (as described above), the energy of the particle surfaces involved in the inter-particulate bonding is a fundamental factor for the tensile strength of such solid bodies. Numerous papers discussing material factors controlling the powder compactibility can be found in the literature, covering aspects such as the dimensions and the compression behaviour of the particles (1). However, few reports have specifically discussed the relationship between powder compactibility and particle surface energy (7–9). Sakr and Pilpel (10) compacted lactose particles coated with surfactants and they reported that an increasing concentration of surfactant decreased the tablet tensile strength, most profoundly at low concentrations. In a report by El Gindy and Samaha (11), a

[1] Department of Pharmacy, Uppsala University, Box 580, 751 23 Uppsala Sweden.
[2] Department of Engineering Sciences, The Ångström Laboratory, Uppsala University, Box 534, 75121 Uppsala, Sweden.
[3] The School of Pharmacy, University of London, 29/39 Brunswick Square, London WC1N 1AX, UK.
[4] To whom correspondence should be addressed. (e-mail: denny.mahlin@farmaci.uu.se)

nearly linear relationship between the surface free energy (literature values) of a series of powders and the tensile strength of tablets formed from them was found. However, since the pressure of formation was constant (90 MPa) during their experiments, tablets of different porosity were obtained for the different materials and, hence, different microstructures of the compacts used can be expected. Recently, Li *et al.* (12) found a relationship between adhesion force, assessed by atomic force microscopy, and the tensile strength of tablets of some materials.

A study of the relationship between surface energy and compactibility of powders should ideally involve the comparison of the tensile strength of tablets with similar microstructures but formed from particles with different surface energies. A possible means to prepare such a series of tablets is to compact amorphous particles produced by spray drying of a solution of a tablet filler alone or of the filler and a surfactant combined. Presumably, the surface energy of the formed particles will be reduced by the addition of a small proportion of the surfactant. A suitable filler is lactose since spray dried lactose particles are spherical in shape and they compress mainly by irreversible particle deformation, i.e. the original particle surfaces are involved in particle–particle bonding (13,14). Also, as indicated earlier (15), the bonding ability of lactose particles can be modified by the addition of a surfactant to the spray feed solution. Hence, the objective of this paper was to study the effect of surface energy, modulated by a surfactant, on the compactibility of amorphous lactose particles prepared by spray drying.

MATERIALS AND METHODS

Materials

Lactose (α-lactose monohydrate, Pharmatose 200 M, DMV, the Netherlands). Polysorbate 80 (polyoxyethylenesorbitan monooleate, Sigma-Aldrich Chemie GmbH, Germany). Magnesium stearate powder (Kebo, Sweden). Penaut oil (Arachidis Oleum, Ph. Eur., Apoteket, Sweden).

Probes. Methane, *n*-hexane (Analytical reagent, Fisher Scientific Ltd), *n*-heptane (HPLC Grade, Fisher Scientific Ltd), *n*-octane (GPR grade, VWR International Ltd), *n*-nonane (Acros Organics, UK), *n*-decane (GPR grade, VWR International Ltd), chloroform (HPLC Grade, Fisher Scientific Ltd), ethanol (HPLC Grade, Fisher Scientific Ltd), ethyl acetate (HPLC Grade, Fisher Scientific Ltd), and acetone (GLC Pesticide residue grade, Fisher Scientific Ltd).

Preparation of Powders

Three different powders consisting of only lactose or of lactose and a small proportion of polysorbate 80 were prepared by spray drying. A solution containing 1% (*w*/*w*) polysorbate 80, prepared with deionised water as a solvent, was added to pre-weighed lactose powders whereby lactose/surfactant mixtures containing 0.001% and 0.01% (*w*/*w*) polysorbate 80 was obtained. Lactose without additive and the lactose/surfactant mixtures were then dissolved in deionised water to a final solid material/water mass ratio of 1:28. The lactose solutions were kept under agitation for 24 h and then spray-dried in a counter-current spray dryer (Niro Atomizer A/S, Denmark), equipped with a rotary atomizer. A peristaltic pump (Watson Marlow 505S, England) at a relative feed rate of 6–7 was used to supply the atomizer with the solution. The inlet and outlet temperatures were 190±5°C and 96±5°C, respectively. The obtained powders were stored in an evacuated desiccator at 0% RH (P_2O_5) for at least 10 days until the moisture content was constant. To check the amount of remaining moisture after the conditioning, the moisture content of all powders was determined as the weight loss of powder samples of approximately 300 mg exposed to 150°C for 10 min using a Halogen Moisture Analyzer (HR73, Mettler Toledo, Switzerland). The moisture content was similar for all powders and of about 2% by weight.

Solid State Properties

Apparent Particle Density

For each powder the apparent particle density (also referred to as the gas pycnometric density and true density of particles) was determined using a helium pycnometer (AccuPyc 1330, Micromeritics, USA; $n=3$).

Solid State Structure

The different powders were analysed by X-ray diffraction using a Diffraktometer D5000 (Siemens, Germany) equipped with a scintillation detector, using Cu-Kα radiation, 45 kV and 40 mA. The samples ($n=1$) were scanned in steps of 0.2° from 6° to 30° (2θ).

Differential Scanning Calorimetry (DSC)

For thermal analysis a Seiko DSC 220 differential scanning calorimeter (SSC/5200 h, Seiko, Japan) was used. Three samples of each powder (0.99–4.68 mg) were weighed into aluminum pans and covered with a lid, which was perforated using a pin. An empty pan was used as reference. Experiments were performed in a dry nitrogen atmosphere at temperatures from 20°C to 300°C using a heating rate of 5°C/min. The instrument was calibrated using indium, tin and gallium.

Surface Energy

Measurements of the surface energy of the spray-dried powders was done using inverse gas chromatography (IGC, Surface Measurement Systems Ltd., UK) by eluting a range of polar and non-polar probes. The non-polar probes used were methane as the inert reference and the hydrocarbons *n*-hexane, *n*-heptane, *n*-octane, *n*-nonane and *n*-decane to determine the dispersive surface energy. The polar probes used were chloroform and ethanol which are predominantly acidic in nature, and ethyl acetate and acetone which are basic.

Each material was packed into pre-silanated glass columns (Surface Measurement Systems Ltd., UK) and tapped for 5 min until a homogenous powder plug was formed which was visually free of any cracks or channels. The

columns were sealed at both ends by silanised glass wool to support the powder samples and conditioned for 2 h at 0% RH by means of a 10 ml/min flow of dry nitrogen gas. The column temperature was kept at 30°C throughout preconditions and experiments. Each probe was injected at 4% (*v*/*v*) whereby a flow rate of 10 ml/min gave a good balance between the speed of elution, the shape of solute peaks and the pressure drop across the column. The retention time was taken as the time elapsed from point of injection to peak maximum. Each packed column was consecutively exposed to all the probes once. The whole procedure was repeated four (powders with polysorbate 80) or seven times (pure lactose).

To find the dispersive surface energy, data analysis was performed as described by Columbano *et al.* (16) where the dispersive surface energies of the powders $\left(\gamma_s^D\right)$ was obtained from plotting $RT\ln V_n$ over $\left(\gamma_L^D\right)^{1/2}$ of the non-polar probes and applying the equation

$$RT\ln V_n = a\left(\gamma_L^D\right)^{1/2} 2N\left(\gamma_s^D\right)^{1/2} + C$$

where R is the gas constant, T the absolute temperature, V_n the retention volume, a the surface area of the probe molecule, γ_L^D the dispersive surface energy of the probe and C a constant.

The $RT\ln V_n$ values of the polar probes diverge from this linear relationship due to specific acidic and basic polar interactions whose magnitude (the deviation on *y*-scale) is equal to the specific energy of interaction $\left(\Delta G_A^{SP}\right)$. Hence, ΔG_A^{SP} could be determined for each polar probe and used to calculate the acidic polar interaction values (K_a) and basic polar interaction values (K_b) of the powders from the gradient and intercept of the linear form plot of

$$\Delta G_A^{SP} = K_a DN + K_b AN^*$$

where AN* is the corrected Lewis acid acceptor number and DN the Lewis base donor number for the different probes (17,18).

Particle and Powder Properties

Particle Size

Particles were suspended in a drop of peanut oil and inspected using an optical light microscope (Olympus Vanox, Japan) equipped with a CCD camera (Olympus DP50) at a magnification of 100×. Digital pictures were taken and the particle size was estimated.

Particle Specific Surface Area

Air permeametry was used to determine the volume specific surface area of the powders (n=3). Samples of each powder were poured into a sample holder and compressed manually to a porosity of approximately 50%. The sample holder was connected to a Blaine apparatus and the time needed for a known volume of air to pass through the powder bed was measured (n=3) (19). The volume specific surface area was calculated using the slip flow corrected Kozeny–Carman equation (20).

Powder Bulk Density

A variable amount of each powder (1.1–4.5 g) was poured into a graduated 10 ml cylinder (20°C, graduation 0.1 ml) using a funnel. The bulk density was calculated from the volume and the weight of the powder (n=5).

Compression Properties

Equipment

A materials testing machine (Zwick//Roell Z100, Germany) equipped with flat-faced circular punches (diameter of 11.3 mm) was used to compress the powders. The movable upper punch was connected to a 100 kN load cell and its position was recorded using an external displacement transducer. The lower punch and die were stationary and mounted to the lower grip. At a pre-load of 2 N, compression speed was set to 25 mm/min. At a force of 100 N data collection started. The upper punch position and pressure data were monitored and collected by the software "testXpert V11.0" and saved in intervals of 10 N. To assess the elastic deformation of the punches and the punch holder, punch deformation curves were recorded by pressing the punches against each other at the compression speed used in the experiments. System deformation data (n=3) was recorded and force–displacement curves were plotted. Except for the initial part at low pressures the force (y) –displacement (x) curves showed linearity. The equation $y = k_a x + l_a + l_b e^{(-k_b x)}$ where the exponential term accounts for the initial curvature was fitted to the deformation data and values for k_a, k_b, l_a, and l_b were obtained. The punch displacement data obtained from powder compression were corrected for the system deformation error, calculated with the above equation, to assess the correct compact height. The system deformation was approximately 0.5 μm/MPa.

Heckel Parameter

An amount of 300 mg powder was manually poured into the die and compressed by applying a maximum pressure of 300 MPa (n=2). The compression parameter P_y, often denoted the yield pressure, was derived from the Heckel equation (21,22):

$$\ln\left(\frac{1}{\varepsilon}\right) = \frac{P}{P_y} + \text{intercept} \quad (1)$$

where ε is the porosity of the compressed powder bed at applied pressure P. P_y was determined by linear regression for pressures between 50 and 150 MPa. The in-die yield pressure ($P_{y\ in}$) was derived from compression profiles recorded by the materials testing machine described above. The out-of-die yield pressure ($P_{y\ out}$) was obtained by using tablet porosity data from tablets prepared with the Korsch press, see below.

Elastic Recovery

The percentage of axial expansion of a compact in die is described by the elastic in-die recovery (ER). It was calculated from the tablet height at 2 N (h_{2N}), the pressure

Table I. Characteristics of Powders (5% Confidence Intervals within Parenthesis)

Material	Apparent particle density (g/cm^3)	Bulk density (g/cm^3)	Powder surface area (cm^{-1})	Glass transition temperature[a] (°C)
Lactose	1.5218 (0.0007)	0.477 (0.030)	7409 (227)	114.7 (0.3)
Lactose/polysorbate 80 0.001% (*w*/*w*)	1.5170 (0.0006)	0.479 (0.031)	7431 (428)	115.4 (0.3)
Lactose/polysorbate 80 0.01% (*w*/*w*)	1.5160 (0.0016)	0.493 (0.021)	7441 (488)	115.4 (0.7)

[a] Midpoint of step change

at which the upper punch is considered to lose contact with the powder bed surface on its upward movement, and the height at maximum pressure ($h_{\text{at pressure}}$) according to following equation:

$$ER(\%) = \frac{h_{2N} - h_{at\ pressure}}{h_{at\ pressure}} \times 100 \quad (2)$$

Reported values are the mean of two measurements of each tablet height.

Permeability Coefficient and Volume Specific Surface Area of Tablets

The materials testing machine described above was used to apply a pressure of 80 MPa to the different powders (n=3). An amount of 500 mg powder was poured into a special die that could be connected to a Blaine apparatus as described earlier (20). After compression the time needed for a known volume of air to pass through the compressed powder bed was measured (n=3). The permeability coefficient (P_c) was calculated using the following equation:

$$P_c = \frac{\ln\left(\frac{h_2}{h_1}\right) La_m}{At \times 2\delta g} \quad (3)$$

where h_2 and h_1 are the start and stop points on the manometer arm, L is the height of the compact, a_m the cross-sectional area of the manometer, A the cross-sectional area of the compact, t the time for air flow, δ density of the manometer liquid and g the standard acceleration of gravity. The distance between the punches at 2 N during the upward movement of the upper punch was chosen as compact height L.

The volume specific surface area of the tablets was calculated using the slip flow corrected Kozeny–Carman equation (20).

Characterisation of Tablet and Fracture Surfaces

The materials testing machine was used to form two 300 mg-tablets of each powder at a pressure of 140 MPa. One tablet of each material was fractured using a materials testing instrument (Holland C50, UK) operated at a loading rate of 1 mm/min. The obtained tablets and tablet fragments were stored at 0% RH for 5 days before images of the upper tablet surfaces and the fracture surfaces were taken with an environmental scanning electron microscope (XL 30 ESEM-FEG, FEI/ Philips, The Netherlands).

Compactibility

Preparation of Tablets

Tablets of 300 mg each were prepared with an instrumented single punch press (Korsch EK 0, Germany) equipped with circular (diameter of 5.65 mm) flat-faced punches at a series of different compaction pressures between 80 and 1,000 MPa. A small paintbrush was used to pre-lubricate the punch and die surfaces by spreading of magnesium stearate powder. During compression the lower punch was stationary and the upper punch machine driven, i.e. when the upper punch was in its upper most position relative to the die the machine was started. For each tablet the maximum compaction pressure was recorded and a variation in compaction pressure of ±5% of the nominal value was accepted (n=3).

Characterisation of Tablets

The porosity of each tablet (ε_t) was calculated from the apparent particle density (ρ_{app}) and the diameter (D), height (h_t) and weight (w) of the tablets in the following way:

$$\varepsilon_t = 1 - \frac{4w}{\pi h_t D^2 \rho_{app}} \quad (4)$$

A materials testing instrument (Holland C50, UK) was used to determine the compression force (F_t) needed to

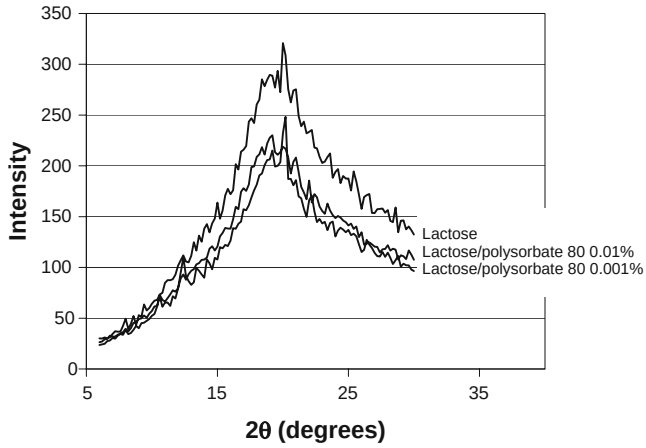

Fig. 1. X-ray diffraction of lactose, lactose containing 0.001% polysorbate 80 (*w*/*w*) and lactose containing 0.01% polysorbate 80 (*w*/*w*).

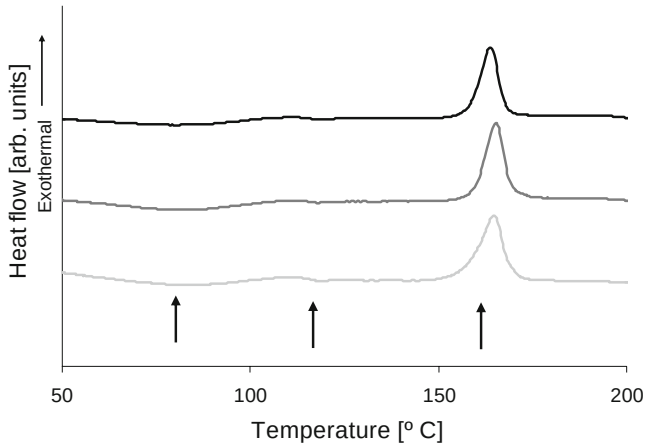

Fig. 2. DSC thermograms of spray-dried powders. Lactose (black), lactose/polysorbate 80 0.001% (*w/w*) (*grey*) and lactose/polysorbate 80 0.01% (*w/w*) (*light grey*). Water loss (broad endotherm, *left arrow*), glass transition (step transition, *mid arrow*) and crystallisation (exotherm, *right arrow*) are essentially identical for the different powders.

fracture the tablets along their diameter. The materials testing instrument was operated at a loading rate of 1 mm/min. The tensile strength of the tablets (σ_t) was thereafter derived according to (23), i.e.:

$$\sigma_t = \frac{2F_t}{\pi h_t D}. \quad (5)$$

RESULTS

Solid State Properties

The differences in apparent particle density between the powders were small (see Table I) but ANOVA analysis showed that the addition of polysorbate 80 had a significant effect on the apparent particle density ($F_{2,16}$=33.709, $p<$ 0.001). The X-ray diffraction diagrams (Fig. 1) showed generally similar and diffuse patterns. The thermograms recorded by DSC showed a step change at approximately 115°C (Fig. 2), which was interpreted as the glass transition of amorphous lactose and accords with values reported in the literature (15). The thermograms also showed an exothermic reaction at higher temperature (164–166°C) that was due to crystallisation of the amorphous lactose. The enthalpy of crystallisation was between 103 and 112 J/g for all samples which is in accordance with the transition energy values found for the crystallisation for 100% amorphous lactose (24).

Inverted gas chromatography provides data (Table II) describing the surface energy in terms of its fundamental components, i.e. the dispersive surface energy and the specific surface energy. Whereas the former is given as unit energy per surface area, the latter is described by the magnitude of dimensionless acidic and basic polar interaction values (K_a and K_b, respectively).

For the dispersive surface energy, the general trend was that it decreased with an increased amount of polysorbate 80 in the powder (Table II). ANOVA showed that the decrease in dispersive surface energy was statistically significant ($F_{2,\ 12}$= 10.334, $p<0.01$) for the powders with surfactant, compared to the spray dried lactose powder without surfactant, for both 0.001% and 0.01% polysorbate 80 ($p<0.05$ and $p<0.01$, respectively). However, an increase in surfactant concentration from 0.001% to 0.01% polysorbate 80 gave no significant decrease in dispersive surface energy.

Concerning the polar interaction values K_a and K_b (Table II), the values showed relatively small differences and no general trend with regard to the dependence of the polysorbate 80 concentration. Hence, the contribution from specific interactions to variations in the overall surface energy was considered negligible.

Particle and Powder Properties

Light microscopy observations showed that the particles of all three powders were smooth and nearly spherical, i.e. particles of all powders were of similar shape. ANOVA analysis did not indicate any significant effects of the addition of low proportions of polysorbate 80 on the bulk density and the volume specific surface area of the powders.

Compression Properties

For all powders, tablet porosity decreased with increasing compaction pressure in a non-linear way. The tablet porosity–compaction pressure profiles coincided for all powders used (Fig. 3). In the compaction pressure interval 50–150 MPa, both the in-die and out-of-die Heckel plots were linear (out-of-die: $r^2>0.98$, in-die $r^2>0.99$) and the Heckel parameter (P_y) was determined by linear regression (Table III). The yield pressure values obtained from in-die analysis were lower than the yield pressure values obtained from out-of-die analysis. Within each group, in-die and out-of-die, the yield pressure values were of the same order of magnitude and no trend regarding the effect of the different proportions of polysorbate 80 on the yield pressure was obtained.

For all tablets, the elastic in-die recovery was between 1.56% and 2.10% (Table III). No relationship between the different proportions of polysorbate 80 and the extent of elastic in-die recovery was obtained.

The permeability to air of tablets compacted at 80 MPa (Table III) was similar for all powders and the ANOVA analysis showed no significant difference in permeability of the tablets.

Table II. Surface Energy Data from IGC Analysis (5% Confidence Intervals within Parenthesis)

Material	Dispersive surface energy (mJ/m^2)	Polar interaction value, K_a	Polar interaction value, K_b
Lactose	49.11 (0.49)	0.0969 (0.0028)	0.0496 (0.0043)
Lactose/polysorbate 80 0.001% (*w/w*)	47.91 (0.57)	0.0939 (0.0042)	0.0479 (0.0084)
Lactose/polysorbate 80 0.01% (*w/w*)	46.30 (1.61)	0.0905 (0.0019)	0.0556 (0.0059)

Table III. Characteristics of Powder Compression Properties (5% Confidence Intervals within Parenthesis)

Material	P_y in die (MPa)	P_y out of die (MPa)	Tablet permeability coefficient[a], $(Ns^2/m)\times10^5$	Tablet surface area[a] (cm^{-1})	Elastic recovery (in die) (%)
Lactose	117.9	209.1	1.127 (0.0190)	7419 (142)	1.62
Lactose/polysorbate 80 0.001% (*w*/*w*)	108.5	219.6	1.168 (0.1181)	6828 (127)	2.10
Lactose/polysorbate 80 0.01% (*w*/*w*)	127.7	219.7	1.154 (0.0681)	7034 (33)	1.56

[a] For tablets formed at 80 MPa

However, for the specific surface area deduced from the air permeability data, the surface area of tablets formed from powders containing polysorbate 80 was lower compared to the lactose tablets (Table III). The ANOVA analysis showed a significant effect ($F_{2,\ 6}$=27.609, p<0.001) of the composition of the powders for the derived specific surface area of the tablets.

Scanning electron microscopy (SEM) images of the upper tablet surface (Fig. 4) were similar for tablets of all powders. Individual particles, deformed at the contact points could be distinguished and cracks, propagating from the edges of the particles towards the centre, were observed. The SEM images of the fracture surface of the tablets (Fig. 5) indicated that particles may also have fused together during compression and, thus the original structure of the particles was partially lost. However, it is possible that some of the particles were fractured during the fracturing of the tablet (25).

Compaction Properties

The compactibility of a powder is often described by the evolution in tablet tensile strength with compaction pressure (Fig. 6) or by the relationship between tablet tensile strength and tablet porosity (Fig. 7). The latter relationship is here presented as a plot of the logarithm of tensile strength over porosity.

Above a critical compaction pressure needed to form a coherent tablet strong enough to be handled, the tensile strength increased with an increased compaction pressure up to a pressure of about 400 MPa (Fig. 6). Thereafter, with increasing compaction pressure, the tablet tensile strength levelled out and, for the powder with 0.01% polysorbate 80, decreased at the highest pressure. The overall compactibility profile tended to be sigmoidal in shape.

The progression of the compactibility profiles at low compaction pressures indicate that with an increased proportion of polysorbate 80 of the powders, an increased compaction pressure was required in order to produce a coherent tablet, (see inset in Fig. 6). In a pressure region between this critical formation pressure and a pressure of about 400 MPa, the compactibility profiles were similar and can be described as displaced in parallel along the pressure axis. Thus, an increased proportion of polysorbate 80 of the powders gave a markedly reduced tablet tensile strength at a given compaction pressure. At the highest compaction pressures used, the profiles tended to merge and no effect of the composition of the powder for the maximum tablet tensile strength, i.e. the level of the plateaus, was observed. The plateau region of the compactibility profile was also associated with an increase in the variability in tablet tensile strength.

The tablet tensile strength generally reduced with increasing tablet porosity (Fig. 7). However, at the lowest porosity values obtained, the profiles levelled out and the tablet tensile strength became more or less independent of tablet porosity, resulting in a merger of the compaction profiles. In the upper half of the porosity range, i.e. from the highest tablet porosities obtained down to a tablet porosity of about 0.15, the profiles are clearly separated and displaced along the *y*-axis almost in parallel. In this porosity range, an increased proportion of polysorbate 80 of the powders gave a markedly reduced tablet tensile strength at a given tablet porosity.

DISCUSSION

Solid State, Powder and Compression Properties of Powders

The particles of all three batches were smooth, nearly spherical microparticles of similar specific surface areas, i.e. the size and the shape of the particles of all three powders were similar and independent of the composition. The solid state properties, except for the dispersive surface energy, were equal or similar between all three powders, which mean that all powders appeared to be completely amorphous. However, a significant although minute difference between the powders in apparent particle density was obtained. It has earlier been shown (26) that amorphous lactose particles prepared by spray drying may be porous (a hollow particle structure), i.e. there may be some internal pores present that affects the determined particle density. The total volume of those pores may vary slightly among the three types of particles. Thus, the obtained small difference in apparent particle density may reflect the complexity of the structure of

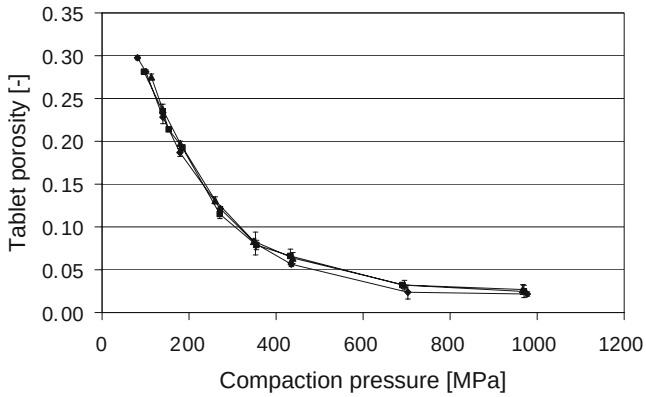

Fig. 3. Tablet porosity–compaction pressure profiles of the different lactose powders. *Diamonds*, lactose; *squares*, lactose/polysorbate 80 0.001% (*w*/*w*); *triangles*, lactose/polysorbate 80 0.01% (*w*/*w*), the *error bars* indicate the standard deviations.

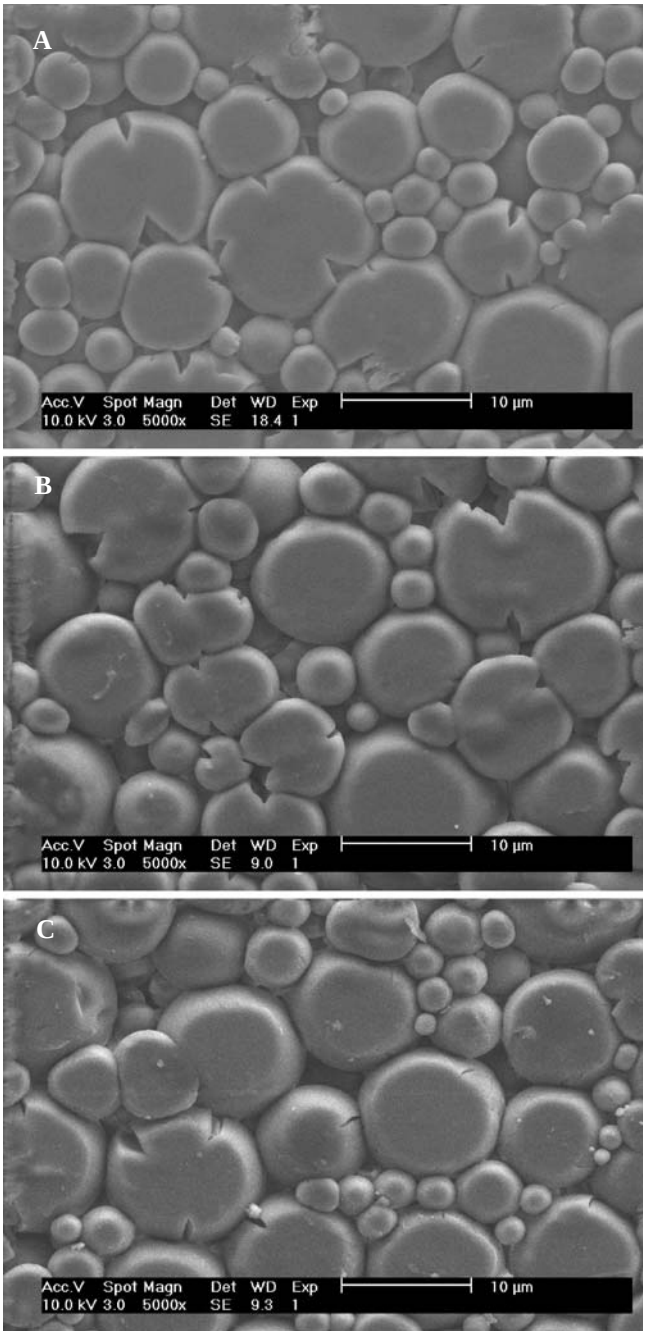

Fig. 4. SEM images of the tablet surfaces (140 MPa), magnification 5,000×. **A** Lactose, **B** lactose/polysorbate 80 0.001% (*w*/*w*) and **C** lactose/polysorbate 80 0.01% (*w*/*w*).

an amorphous particle prepared by spray-drying rather than indicate a difference in degree of amorphicity.

Regarding the dispersive surface energy, the general trend was that the surface energy continuously reduced with an increased proportion of polysorbate 80 in the powders. The reduction in surface energy is assumed to be due to an alteration of the particles surface composition, caused by the adsorption of surfactant to the air–water interface of the droplets during spray drying. The particle formation process in terms of migration and local concentration fluctuations of the components is a too complex issue to be understood in detail here. For instance, a possible self aggregation of the surfactant (i.e. the critical micelle concentration) and its relation with the adsorption to droplet surface is likely to be affected by temperature, carbohydrate concentration and the surface to volume ratio of the spray. In any case and importantly for this study, the preparation of three types of particles with similar particle and solid state properties, but with various surface energies, was accomplished.

A possible means to describe the degree of particle fragmentation that occurs during compression is to study the

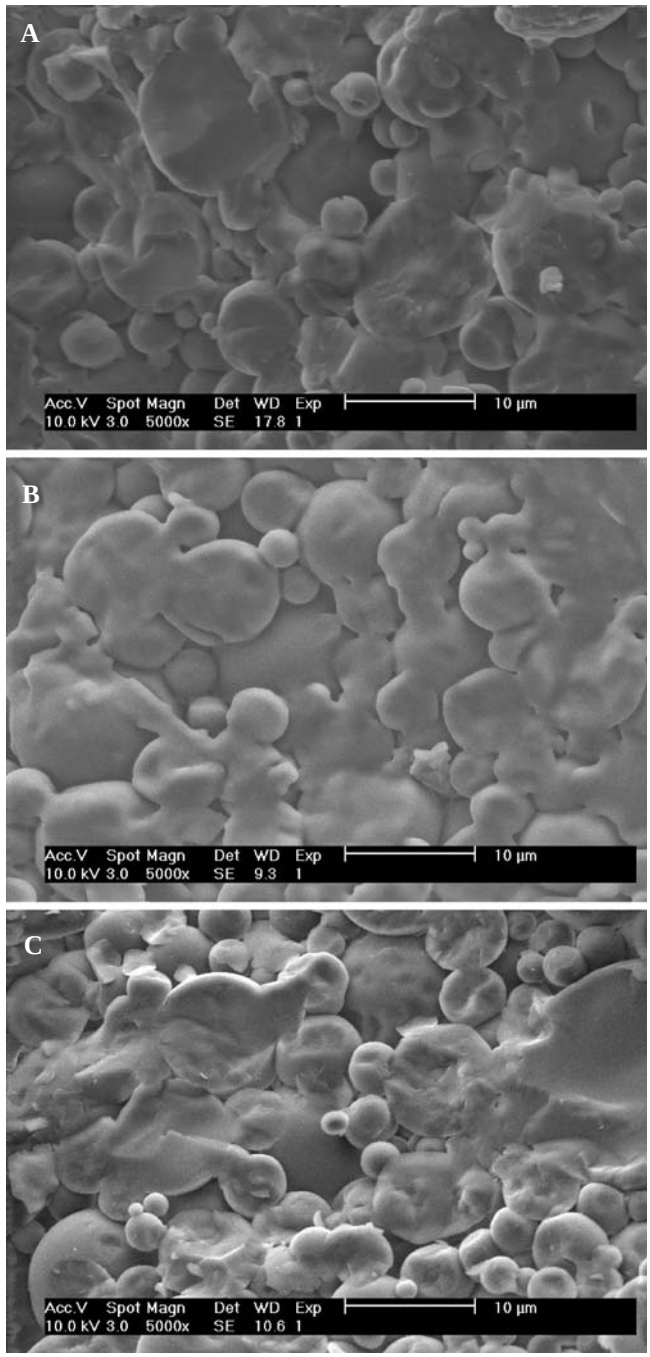

Fig. 5. SEM images of the fractured surface (140 MPa), magnification 5,000×. **A** Lactose, **B** lactose/polysorbate 80 0.001% (*w*/*w*) and **C** lactose/polysorbate 80 0.01% (*w*/*w*).

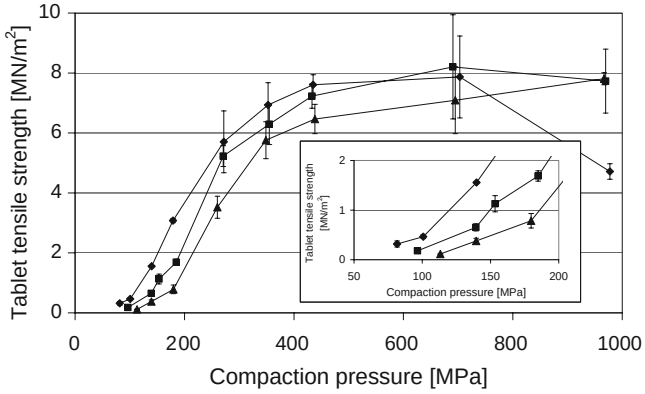

Fig. 6. Effect of compaction pressure on tablet tensile strength. *Diamonds*, Lactose; *squares*, lactose/polysorbate 80 0.001% (*w*/*w*); *triangles*, lactose/polysorbate 80 0.01% (*w*/*w*), the *error bars* indicate the standard deviations. Inset shows blow up of low pressure region.

change in specific surface area with compaction pressure (20). For all powders, the original powder surface area and the surface area of tablets compacted at 80 MPa were similar. Thus, fragmentation of particles during tableting was limited and particle deformation dominated the compression process, which is consistent with earlier reports (13,15). One can note, however, that the surface areas of tablets formed from the two lactose powders containing polysorbate 80 were slightly reduced in comparison with the corresponding specific powder surface areas.

The SEM images of the upper surfaces of the tablets indicate that the tablets formed from all three powders were agglomerates of small particles whose size are similar to the original particles. The particles deformed and cracked during compression but the SEM images support that the incidence of particle fragmentation during compaction was limited. The observed structure of the tablets compare favourably with earlier experiences on the structure of tablets produced from amorphous lactose (13,15). The SEM images of the fracture surfaces are more complicated to interpret since the propagation of the crack during failure of the tablet may cause fracturing of the particles (25). Nevertheless, the images support that the tablets of all powders generally were

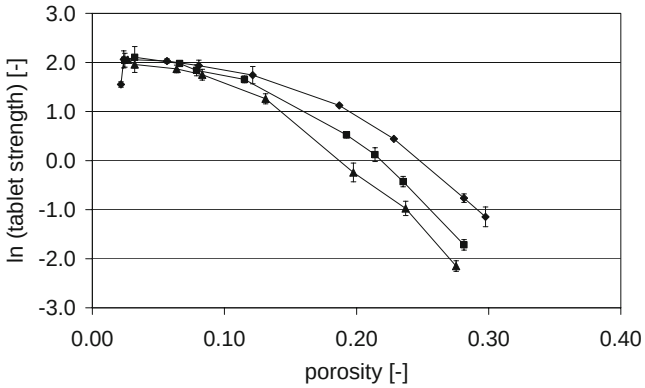

Fig. 7. Effect of tablet porosity on the tablet tensile strength. *Diamonds*, Lactose; *squares*, lactose/polysorbate 80 0.001% (*w*/*w*); *triangles*, lactose/polysorbate 80 0.01% (*w*/*w*), the *error bars* indicate the standard deviations.

agglomerates of similar structure. Furthermore, observations of some particles being fused locally during the compression process indicate that solid bridges were formed during compression. A similar observation has been reported earlier (14) for tablets produced from amorphous lactose particles, especially for tablets formed at relatively high compaction pressures. Thus, in the tablets, two types of inter-particulate bonding can be expected: intermolecular forces acting between surfaces at the inter-particulate junctions, and solid bridges formed by mixing of solid phase at the particle–particle interface. The formation of solid bridges may explain the lower surface area for tablets compared to the uncompacted powders, which was detected when polysorbate 80 was present. The reason for an increase in solid bridge formation for powders containing the surfactant may be attributed to enhanced possibility for local particle–particle fusion. It appears that polysorbate 80, preferentially located at the particle surface, increased the mobility of the molecules at the surface of the particles, promoting fusion at high pressure contacts between particles surfaces. Hence, it is also likely that the incidence of solid bridges in the tablets increases with increased compaction pressure.

Since the tablet porosity–compression pressure profiles coincided for the three powders and the permeability coefficients as well as the images were the same for the tablets of all powders, it can be concluded that different powders showed similar compression behaviour. As discussed above, particle deformation dominated the compression process of these powders and the elastic and plastic deformability of the particles, as evaluated by the elastic recovery of the tablets and the Heckel parameter, were similar between the powders.

The objectives with the powder preparation procedure were, firstly, that the particles of all three powders should possess such solid state, powder and compression properties that the tablets formed from them could be expected to be of similar microstructure and, secondly, that the surface energy of the particles should vary with proportion of polysorbate 80. It is concluded that these two criteria were sufficiently met by the particle preparation procedure used. It is also concluded that in a significant portion of the compaction pressure range used, particle–particle bonding in the tablet involved predominantly original particle surfaces. The particles fragmented or fused during compression only to a limited extent. However, at high

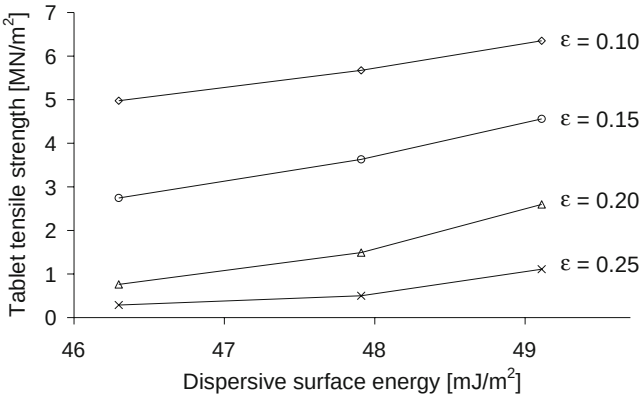

Fig. 8. Effect of surface energy on the tablet tensile strength at four different tablet porosities (ε, as indicated in the diagram).

compaction pressures particle–particle bonding by solid bridges seemed to increase substantially.

Powder Compactibility

In this study, the compactibility of the powders was evaluated in terms of the relationship between the tablet tensile strength and compaction pressure, and between the tablet tensile strength and tablet porosity (Figs. 6 and 7). In the following discussion, the profiles are somewhat simplistically divided into two parts: A first region, corresponding to compression pressures between about 50 to 400 MPa (tablet porosities between 0.3 and 0.12), and a second region corresponding to compaction pressures above about 400 MPa (tablet porosities below about 0.12).

In the first region, the increase in tablet tensile strength with increasing compaction pressure and decreasing tablet porosity, 'the rate of compactibility,' was almost independent of the composition of the powders used. However, since the compactibility profiles of the powders were displaced in parallel along *x*-axis of the plots the tablet tensile strength was strongly affected by the particle dispersive surface energy at a given compaction pressure or tablet porosity. Expressed alternatively, a reduction in particle dispersive surface energy increased the pressure needed to form a compact of a predetermined tensile strength. Figure 8 shows the relationship between tablet strength and dispersive surface energy at different tablet porosities. It is clear that, at a specific tablet porosity, there is a positive correlation between dispersive surface energy and tablet tensile strength. It is thus concluded that for tablets that are similar in microstructure, the surface energy is a significant factor for the tensile strength of powder compacts. In general terms, the results indicate that the surface energy of particles is one of the fundamental factors that controls the compactibility of powders and can explain why powders show poor compactibility.

In the second region, the compactibility profiles (Figs. 6 and 7) tended to merge and finally the tablet tensile strength became more or less independent of compaction pressure and tablet porosity. For one powder, the tensile strength even decreased. The traditional interpretation of the reduction in tablet tensile strength at high compaction pressures is incipient capping of the tablets (27).

Substantiated by the discussion above on the physical structure of the formed tablets, we suggest that the contact area between particles was controlled by the mechanical properties of the particles. As the powders showed equal mechanical behaviour and micro-structure, the variation of compactibility must be explained by the differences in surface energy. At higher porosities, in the first region of the compactibility profile, it is reasonable that intermolecular forces acting between original particle surfaces, at the inter-particulate contact sites in the tablet, is the tablet strength controlling bonding mechanism. The difference in compactibility in the first region is thereby explained by a reduced strength of the particle–particle bonds due to a reduced dispersive surface energy of the external particle surfaces. Further, since solid bridges appeared to be formed between the particles to an increasing degree with increasing compaction pressure (i.e. at reduced tablet porosity), the formation of solid bridges became of increased importance for the evolution in tablet strength with pressure in the second region. Thus, solid bridges become the tablet strength controlling bonding mechanism in this region and may explain the merging of the compactibility profiles. Thereby, the significance of a difference in original particle dispersive surface energy will diminish and eventually cease.

CONCLUSIONS

In this study, spray dried powders were produced in which the particle surface energy could be modified by the addition of a surface active agent while constant solid state and particle bulk properties were maintained. This procedure provided a model system which enabled studies of the effect of surface energy on powder compactibility.

It was found that the particle surface energy influenced the powder compactibility while the compressibility and the evolution of tablet micro-structure were more or less unaffected. Therefore, we suggest that the micro-structure and, hence, the total inter-particulate contact area per fracture area, was controlled by the mechanics of the particles, but essentially independent of the particle surface energy. Within a normally used tablet porosity range the surface energy of the particles strongly affected the tablet tensile strength. Thus, for a tablet where adsorption bonds is the tablet strength controlling bonding mechanism, a reduced particle surface energy will reduce the strength of adsorption bonds formed between particles during compression and this reduction in bond strength requires a proportional increase in inter-particle contact area if a tablet of a predetermined tensile strength should be formed. However, for a tablet where solid bridges is the tablet strength controlling bonding mechanism, the tablet strength will be almost unaffected by the particle surface energy.

In conclusion, the preparation of particles by spray drying with a surfactant dissolved in the feed solution provides the formulation scientist with an opportunity to control surface interactions between particles without affecting their mechanics.

ACKNOWLEDGEMENTS

This study is a part of a project supported financially by The Swedish Foundation for Strategic Research and AstraZeneca, Sweden. Nils-Olov Ersson, Department of Material Chemistry, Ångström Laboratory, Uppsala, is gratefully acknowledged for performing the X-ray powder diffraction analysis and Dr Hardyal S Gill, School of Pharmacy, University of London, for the IGC analysis.

REFERENCES

1. G. Alderborn. The effect of particle size and shape on the compactibility of powders. In G. Alderbor and C. Nyström (eds.), *Pharmaceutical Powder Compaction Technology*, Marcel Dekker, New York, 1996.
2. M. Abdel-Ghani, J. G. Petrie, J. P. K. Seville, R. Clift, and M. J. Adams. Mechanical-properties of cohesive particulate solids. *Powder Technol.* **65**:113–123 (1991).
3. K. Kendall. Agglomerate strength. *Powder Metall.* **31**:28–31 (1988).

4. M. A. Mullier, J. P. K. Seville, and M. J. Adams. A fracture-mechanics approach to the breakage of particle agglomerates. *Chem. Eng. Sci*. **42**:667–677 (1987).
5. H. Rumpf. *The Strength of Granules and Agglomeration*. Interscience, New York, 1962.
6. J. Israelachvili. *Intermolecular and Surface Forces*. Academic, London, 1992.
7. P. G. Karehill and C. Nystrom. Studies on direct compression of tablets. 21. Investigation of bonding mechanisms of some directly compressed materials by strength characterization in media with different dielectric-constants (relative permittivity). *Int. J. Pharm.* **61**:251–260 (1990).
8. M. Luangtana-Anan and J. T. Fell. Bonding mechanisms in tabletting. *Int. J. Pharm*. **60**:197–202 (1990).
9. H. Olsson, A. Adolfsson, and C. Nystrom. Compaction and measurement of tablets in liquids with different dielectric constants for determination of bonding mechanisms—evaluation of the concept. *Int. J. Pharm*. **143**:233–245 (1996).
10. F. M. Sakr and N. Pilpel. The tensile-strength and consolidation of lactose coated with non-ionic surfactants. 2. Tablets. *Int. J. Pharm.* **10**:57–65 (1982).
11. N. A. El Gindy and M. W. Samaha. Tensile-strength of some pharmaceutical compacts and their relation to surface free-energy. *Int. J. Pharm*. **13**:35–46 (1982).
12. Q. Li, V. Rudolph, B. Weigl, and A. Earl. Interparticle van der Waals force in powder flowability and compactibility. *Int. J. Pharm*. **280**:77–93 (2004).
13. T. Sebhatu and G. Alderborn. Relationships between the effective interparticulate contact area and the tensile strength of tablets of amorphous and crystalline lactose of varying particle size. *Eur. J. Pharm. Sci*. **8**:235–242 (1999).
14. T. Sebhatu, C. Ahlneck, and G. Alderborn. The effect of moisture content on the compression and bond-formation properties of amorphous lactose particles. *Int. J. Pharm*. **146**:101–114 (1997).
15. J. Berggren, G. Frenning, and G. Alderborn. Compression behaviour and tablet-forming ability of spray-dried amorphous composite particles. *Eur. J. Pharm*. **22**:191–200 (2004).
16. A. Columbano, G. Buckton, and P. Wikeley. Characterisation of surface modified salbutamol sulphate-alkylpolyglycoside micir-oparticles prepared by spray drying. *Int. J. Pharm*. **253**:61–70 (2003).
17. V. Gutmann. *The Donor–Acceptor Approach to Molecular Interaction*. Plenum, New York, NY, 1978, pp. 19–20.
18. F. L. Riddle and F. M. Fowkes. Spectral shifts in acid–base chemistry. 1. Vanderwaals contributions to acceptor numbers. *J. Am. Chem. Soc.* **112**:3259–3264 (1990).
19. R. L. Blaine. *ASTM Bull.* **123**:51–55 (1943).
20. G. Alderborn, M. Duberg, and C. Nystrom. Studies on direct compression of tablets.10. Measurement of tablet surface-area by permeametry. *Powder Technol.* **41**:49–56 (1985).
21. R. W. Heckel. Density–pressure relationship in powder compaction. *Trans. Metall. Soc. AIME*. **221**:671–675 (1961).
22. R. W. Heckel. An analysis of powder compaction phenomena. *Trans. Metall. Soc. AIME*. **221**:1001–1008 (1961).
23. U. Gelius, B. Wannberg, P. Baltzer, H. Fellnerfeldegg, G. Carlsson, C. G. Johansson, J. Larsson, P. Munger, and G. Vegerfors. A new ESCA instrument with improved surface sensitivity, fast imaging properties and excellent energy resolution. *J. Electron. Spectrosc. Relat. Phenom*. **52**:747–785 (1990).
24. A. Gombas, P. Szabo-Revesz, M. Kata, G. Regdon, and I. Eros. Quantitative determination of crystallinity of alpha-lactose monohydrate by DSC. *J. Therm. Anal. Calorim*. **68**:503–510 (2002).
25. F. Nicklasson, B. Johansson, and G. Alderborn. Occurrence of fragmentation during compression of pellets prepared from a 4 to 1 mixture of dicalcium phosphate dihydrate and microcrystal-line cellulose. *Eur. J. Pharm. Sci*. **7**:221–229 (1999).
26. J. Elversson and A. Millqvist-Fureby. Aqueous two-phase systems as a formulation concept for spray-dried protein. *Int. J. Pharm*. **294**:73–87 (2005).
27. E. Shotton and J. Ganderton. The strenght of compressed tablets. III. The relation of particle size, bonding and capping in tablets of sodium chloride, aspirin and hexamin. *J. Pharm. Pharmacol.* **13**:144T (1961).